Petroleum and Coal

Article **Open Access**

MATHEMATICAL MODELING OF DILUTED SPECIES EXTRACTION FROM DRINKING WATER THROUGH A MEMBRANE BIOREACTOR USING STIFF-SPRING METHOD

S. J. Poormohammadian[1], M. Koolivand-Salooki[2], P. Darvishi[1]*, A.M. Ghalambor Dezfuli[3]*

[1] *Chemical Engineering Department, Yasouj University, Yasouj, Iran*
[2] *Gas Research Division, Research Institute of Petroleum Industry, Tehran, Iran*
[3] *Physics Science Department, Shahid Chamran University of Ahvaz, Ahvaz, Iran*

Received September 9, 2017; Accepted December 1, 2017

Abstract

The combination of finite element method (FEM) with stiff-spring method (SSM) was exploited to model the two-dimensional transient transport of diluted species through a membrane bioreactor (MBR) adopted with a hollow-fiber module. The predictions of the model were validated by the experimental data obtained for removal of nitrate from drinking water. Stiff-spring method as a powerful mathematical approach was applied to solve the system of governing equations that were numerically divergent within the ranges of some parameters and had discontinuities in boundary conditions. The effect of equilibrium partition coefficient on membrane efficiency and exit concentration was investigated. It was shown that the model diverged for some values of equilibrium partition coefficient, when non-stiff methods were utilized. On the other hand, when the SSM was used, the results were completely stable and have a good agreement with the experimental data for a wide range of equilibrium partition coefficients. Finally, simulation results confirm that the application of stiff spring method is more reliable and accurate compare to non-stiff spring method.

Keywords: *Finite element method; stiff spring method; water treatment; membrane bioreactor; diluted species.*

1. Introduction

Over the past two decades, membrane filtration has played a major important role in industrial separation processes [1]. Numerous improvements of the technology have allowed membrane selection for a particular process to be done more easily and more quickly. The development of this technology is due to the increasing number of different types of applications of these processes in different domains, particularly in the industrial sector.

A membrane bioreactor (MBR) is a suspended growth activated sludge system which utilizes microfiltration or ultrafiltration membranes for solid/liquid separation [2]. The retention of all suspended matter and most soluble compounds through membrane filtration leads to excellent effluent quality. The benefits of MBRs in municipal wastewater treatment have been adequately described elsewhere [2-3].

Hollow-fiber membrane contactors (HFMCs) have attracted large attentions as a powerful device for the extraction of species through drinking water. A major part of the interest towards HFMCs is due to their capability in setting a dispersion free contact. In addition, the velocities of both phases can be chosen independently without any flooding and unloading problems [4-6]. The mechanism of separation in this kind of membrane contactors is based on the mass transfer between the two phases. This kind of contactors provides considerable extraction [7-9].

There are two approaches for the mass transfer modeling of diluted removal from wastewater using HFMCs. In the first one which is based on the resistance-in-series model, the resistances in the aqueous feed phase, boundary layer, and the membrane phase are

considered in series. In this model the resistance at the shell side is neglected because of instantaneous chemical reaction which occurs between diluted species and extractive solvent. One important factor which affects the resistance of membrane is partition coefficient. Partition coefficient, is defined as the concentration at equilibrium in the solvent phase divided by that in the feed. In hydrophobic membrane expecting that a large value of partition coefficient will increase mass transfer coefficient of membrane beyond the coefficient of the feed. The value of partition coefficient which is based on the choice of membrane properties frequently is justified by experiment [10]. The partition coefficients between the donor phase and the membrane can be measured by some methods with the membrane-coated fiber (MCF) technique [11]. The second approach is based on solving conservation equations for solute in the aqueous feed and membrane phases. In this approach, conservation equations including continuity, energy, and momentum equations are derived and solved simultaneously by appropriate numerical methods.

Computational fluid dynamics (CFD) techniques may provide a lot of useful information for the development of membrane processes. The applications of CFD are usually carried out in three steps: preprocessing, processing, and post processing, respectively. To our knowledge, there are some CFD simulation studies on mass and momentum transfers of ammonia in HFMCs [12-13]. CFD has been widely used to simulate the hydrodynamic behavior of membrane separation processes using membrane modules [14–18]. This method was used to simulate the gas separation and solvent extraction carried out in membrane contactors [19–25]. The obtained results revealed excellent agreement between the experimental and theoretical data, but still there were some difficulties in the convergence of governing equations. Also several methods have been developed for solving the stiff differential equations. Strabrowski [26] suggest an algorithm for solving stiff ordinary differential equations used the Brayton-Gustavson-Hatchel (BGH) method. Mieczyslaw Metzger [27] proposed the discrete response equivalent (DRE) integration algorithms for real-time simulation of biologically activated sludge process with a fixed integration step size, which is independent of the process dynamics. Rodrigo Castro *et. al.* [28] introduces a numerical delay-differential equation solver based on state quantization instead of time slicing. Gustavo Migoni *et al.* [29] present linearly implicit quantization-based integration methods for stiff ordinary differential equations.

In hollow-fiber membrane contactors (HFMCs), the membrane mainly acts as a physical barrier between the two fluids. In this case, unlike most membrane operations, the membrane will not have any effect on partition coefficients. The partition coefficient is supposed to be independent of concentration in other works due to the discontinuity of concentrations in the boundaries [12]. The fluctuations of partition coefficient may cause severe problems in solving the governing equations.

In the present work a numerical technique based on finite element with the aid of stiff-spring method is used to solve the two-dimensional axisymmetric flow field and convective diffusion equation for diluted species transport in laminar flow over a permeable surface of a tubular HFMC. The effects of variations of partition coefficient on the membrane efficiency and exit concentration of the diluted species in the lumen side also have been considered.

2. Mathematical modeling

Computational Fluid Dynamics (CFD) can be used for virtual prototyping of chemical membrane bioreactors. Because it is based on control volume or finite element methodology, the local variations of the fluid, thermal and mass transport properties can be visualized in comparison to simple simulations and it can be used for designing of MBR. Since permeation is based on local conditions near to the membrane face, CFD is the best tool to analyze membrane bioreactors [13].

The model is proposed based on the following assumptions :

- The flow is in isothermal condition
- The fluid is Newtonian and physical properties and transport coefficients are constant
- The flow regime is laminar and the velocity profile in the lumen side is fully developed

- Non-wetted mode exist in which contaminated water fills all the membrane pores
- There are no resistances of concentration polarization layer, cake formation and pore blocking, and accordingly, no changes in the radius of the lumen and shell side during the process.

The membrane bioreactor CFD model that formulates the couples of fundamental mass and momentum balance equations and then solves using numerical techniques such as FEM. These equations are non-linear and cannot be solved analytically in nearly all cases. Thus the equations must be linearized and solved over all the nodes and grids (generated mesh). What is required to define the flow-field is to have the geometry dimensions, boundary conditions, fluid properties and all the needed input data.

The conservation equations for the solute in the contactor were derived and solved to predict the performance of the contactor. The model is developed for a hollow fiber, as shown in Fig. 1. As can be seen, the feed phase flows with a fully developed laminar velocity profile in the lumen side of micro porous hollow fiber membrane. The fiber is surrounded by the solvent which flows in the same direction of the feed phase. Therefore; the membrane contactor system consists of three sections: lumen side, membrane, and shell side. In order to validate the simulation results, experimental data reported by Ergas and Rheinheimer [30] for the extraction of nitrate from aqueous solutions were used. The simulations were carried out at identical conditions employed in conducting experiments.

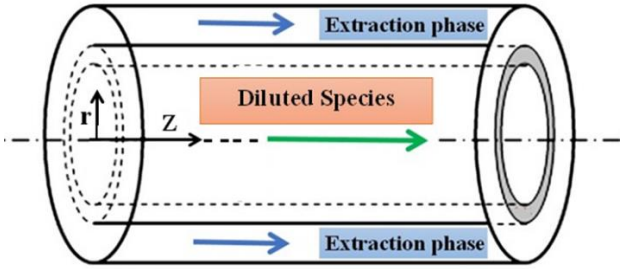

Fig.1 a schematic of hollow fiber membrane with three zones used in the model

2.1. Mass balance for the lumen side

The mass conservation equations for diluted species in the lumen side can be expressed as:

$$\frac{\partial c_L}{\partial t} - D_{ds}\left[\frac{\partial^2 c_L}{\partial t^2} + \frac{1}{r}\frac{\partial c_L}{\partial r} + \frac{\partial^2 c_L}{\partial z^2}\right] = R - V_Z \frac{\partial c_L}{\partial z} \quad (1)$$

Reaction rate(R) is zero because no chemical reaction occurs in the lumen side. The velocity distribution in the lumen side is assumed to follow Newtonian laminar flow:

$$V_Z = 2\bar{u}\left[1 - \left(\frac{r}{r_1}\right)^2\right] \quad (2)$$

The boundary conditions assumed for the lumen side are as follows:

$$c_L = C_0 \qquad at\ z = 0 \quad (3)$$

$$n.(-D_{ds}\nabla c) = 0 \qquad at\ z = L \quad (4)$$

The convective flux boundary condition assumes that all mass passing through this boundary is convection-dominated. This assumes that any mass flux due to diffusion across this boundary is zero.

$$\frac{\partial c_L}{\partial r} = 0 \qquad at\ r = 0 \quad (5)$$

$$c_L = c_M \qquad at\ r = r_1 \quad (6)$$

2.2. Mass balance for the membrane

The mass conservation equation for diluted species diffusive transfer through the membrane can be written as:

$$\frac{\partial c_M}{\partial t} - D'_{ds}\left[\frac{\partial^2 c_M}{\partial r^2} + \frac{1}{r}\frac{\partial c_M}{\partial r} + \frac{\partial^2 c_M}{\partial z^2}\right] = 0 \quad (7)$$

There is no chemical reaction in the membrane, so the reaction term in the membrane is not considered. Since pore diffusion occurs only by ordinary molecular diffusion, Fick's law can be used with an effective diffusivity.

Correlations developed by Koponen *et.al.* [31] is used to approximate the pore-path tortuosity as a function of porosity.

$$\tau = 1 + a\frac{(1-\varepsilon)}{(\varepsilon-\varepsilon_p)^n} \quad (8)$$

$$D'_{ds} = \frac{\varepsilon D_{ds}}{\tau} K_r \quad (9)$$

K_r, the restrictive factor, accounts for the effect of pore diameter on causing interfering collisions of diffusing solutes with the pore wall, when the ratio of molecular diameter to pore diameter exceeds about 0.01.

It should be noted that like the lumen side, the resultant value of the effective diffusion coefficient in the membrane also must be correlated in an anisotropic one for numerical simulation. The boundary conditions for the membrane are given as:

$$n.N = 0; N = -D'_{ds}\nabla c_M \quad at\ z = 0\ and\ z = L \quad (10)$$

$$c_M = c_L\ at\ r = r_1 \quad (11)$$

$$c_M = \frac{c_{sh}}{k} at \quad r = r_2 \quad (12)$$

2.3. Mass balance for the shell side

The mass conservation equation for diluted species in the shell side of the MBR is obtained using Fick's law of diffusion for estimation of diffusive flux:

$$\frac{\partial c_{sh}}{\partial t} - D''_{ds}\left[\frac{\partial^2 c_{sh}}{\partial r^2} + \frac{1}{r}\frac{\partial c_{sh}}{\partial r} + \frac{\partial^2 c_{sh}}{\partial z^2}\right] = R'' - V''_Z\frac{\partial c_{sh}}{\partial z} \quad (13)$$

For cell growth in the biofilm, a good reaction kinetic model should be used. For example bacterial growth kinetics model proposed by Monod as well as the enzyme reaction kinetic model proposed by Michaelis and Menten can be taken into account for denitrification reaction, where the former is used most often to describe the relationship between bacterial growth and substrate concentration [32].

In the MBR, diluted spices flows through the lumen of a hollow fibre micro porous membrane and diffuses through the membrane pores. The reaction of transferring diluted spices takes place on the shell side of the membrane. A concentration difference through the membrane will be induced that creates the driving force for mass transfer. Diffusion is the rate-limiting step in this reaction. If the concentration of diluted species changed then the concentration profile is changed and the reaction plane will be varied. In this way the stoichiometry is maintained due to the introduction of variable diffusion resistances. Thus in this model we suppose the bulk liquid flow (macroscopic point of view) in the shell side takes into account the flow behaviour of liquid which is not affected by the biological reaction. So, the reaction rate expression, R", can be neglected [33]:

In the case of liquid flow, a momentum balance using Navier–Stokes equation is considered. The concentration and velocity distribution are obtained by solving the mass and the momentum equations, simultaneously. In this case, Navier–Stokes and the continuity equations are defined as follows [34]:

$$\rho\frac{\partial V''_Z}{\partial t} + \rho V''_Z.\nabla V''_Z = \nabla.\eta(\nabla V''_Z + (\nabla V''_Z)^T) - \nabla p \quad (14)$$

$$\nabla.V''_Z = 0 \quad (15)$$

The Happel's model was used to estimate the radius of the shell side, r_3 in Fig. 2 [35]. The boundary conditions for the shell side are given as:

- Continuity equation

$$c_{sh} = kc_M \quad at\ r = r_2 \quad (16)$$

$$n.N = 0; N = -D''_{ds}\nabla c_{sh} + c_{sh}V''_Z \quad at\ r = r_3 \quad (17)$$

$$c_{sh} = s(t) \quad at\ z = 0 \quad (18)$$

$$n.(-D''_{ds}\nabla c_{sh}) = 0 \quad at\ z = L \quad (19)$$

- Momentum equation

$V_Z'' = 0$, $No\ slip$ $\quad at\ r = r_2$ (20)

$V_Z'' = 0$, $No\ slip$ $\quad at\ r = r_3$ (21)

$V_Z'' = V_{Z,0}''$ $\quad at\ z = 0$ (22)

$p = p_0$ $\quad at\ z = L$ (23)

In the case of s(t), by putting into practice a large and completely mixed reservoir with constant density connected to the shell side of the membrane module, a mass balance on the reservoir can be written as follows:

$$\frac{d(V_{res}.\ s(t))}{dt} = Q.c(L,r,t) - Q_{res}.s(t) \quad (24)$$

With the initial condition s(t)=0 at time t=0. Neglecting the volume of the pipes with respect to the total volume of the system, the following mass balance for the diluted species provides a relationship between the reservoir and the hollow fiber MBR unit [36]:

$$Q.c_L(L,r,t) = \int_0^{r_1} V_Z(L,r,t)c_L(L,r,t)2\pi r dr \quad (25)$$

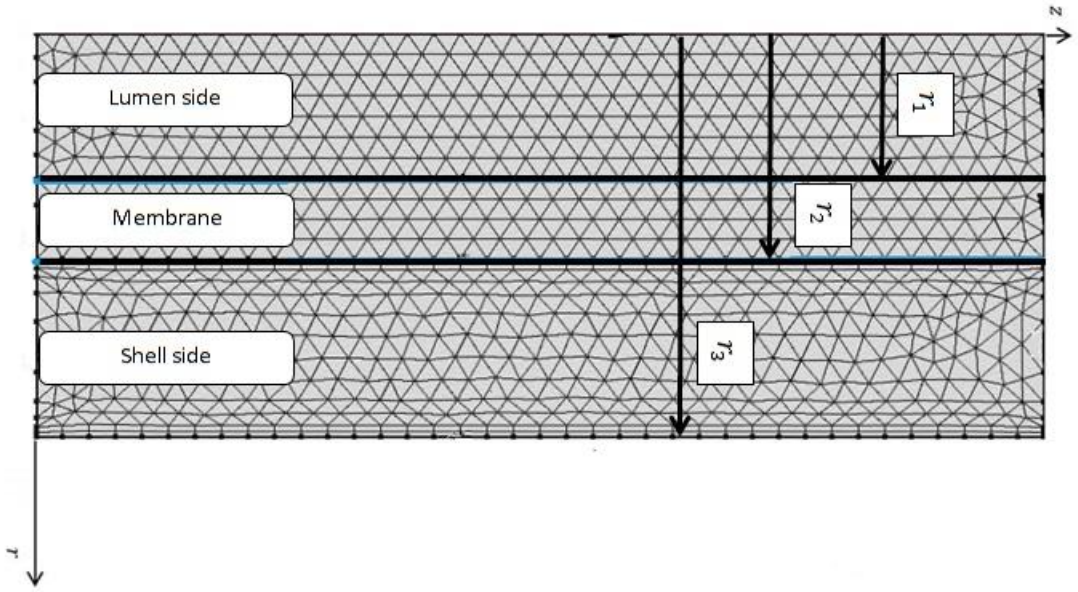

Fig.2. The meshes generated to determine diluted species behavior in extractive MBR

3. Numerical solution methodology

Comprehensive knowledge of fluid dynamics and mass transfer mechanisms in industrial membrane separation processes is crucial for proper apparatus design and optimization. For these reasons, computational fluid dynamics (CFD) methods appear to be very promising, since their application could lead to detailed predictions of membrane separation operations in any geometrical configuration and scale of the modules. Development of proper modelling strategies and strict tests on their predictive capabilities are still required in order to reliably adopt CFD codes as a design tool in this field.

The mentioned equations were solved numerically by using COMSOL Multiphysics software, version 4.3. This software uses finite element method (FEM) for the numerical solutions of equations.

The direct solver UMFPACK was employed because it is preferable for 1D and 2Dmodels. It employs the COLAMD and AMD approximate minimum degree preordering algorithms to permute the columns so that the fill-in is minimized. This solver is an implicit time-stepping scheme, which is well suited for solving stiff and non-stiff non-linear boundary value problems. An INTEL-PC-Core i5 (CPU speed is 3200 MHz) was used to solve the set of equations. The computational time for solving the set of equations was about 5 min. Parameters and physical constants for numerical simulations were taken from literature [12–13].

The meshes generated by COMSOL software are illustrated in Fig.2 To avoid excessive amounts of elements and nodes, scaling factor of 100 was employed in z direction where COMSOL automatically scaled back the geometry after meshing [13]. This generates an anisotropic mesh around 1700 triangular elements. Adaptive mesh refinement in COMSOL, which generates the best and most minimal meshes, was used to mesh the extractive MBR geometry [37].

3.1. Scaling

The aim of scaling is to reduce the number of parameters in a given model. So, a prerequisite of the technique of scaling is knowledge of the equations governing the system.

Scaling does not necessarily yield dimensionless quantities. A scale model is most generally a physical representation of an object, which maintains accurate relationships between all important aspects of the model, although absolute values of the original properties need not be preserved. This enables it to demonstrate some behavior or property of the original object without examining the original object itself.

Since r to z ratio is a very small value, scaling in z direction is necessary to avoid excessive amounts of elements and nodes in the numerical solver. Therefore we have introduced a new scaled z- coordinate, $\hat{z}$, and a corresponding differential for the mass transports:

$$\hat{z} = \frac{z}{scale} \quad (26)$$

$$dz = scale.d\hat{z} \quad (27)$$

In the mass-transport equations, c is differentiated twice in the diffusion term, which implies that the diffusive flux vector's z-component must be multiplied by $(1/scale)^2$. The convective component is only differentiated once, and therefore must be multiplied by $1/scale$. Scaling the diffusive part of the flux could be introduced as an anisotropic diffusion coefficient where the diffusion in the z direction is scaled by the factor $(1/scale)^2$. This gives the following diffusion-coefficient matrix:

$$\bar{D} = \begin{bmatrix} D & 0 \\ 0 & \frac{D}{scale^2} \end{bmatrix} \quad (28)$$

The velocity vector must be multiplied by $1/scale$ to account for the new scaled z-coordinate.

3.2. Stiff-spring method

In particular, stability is of importance. If stability will be lost, then the linearly implicit methods are not suited for solving stiff differential equations. Stiff differential equations arise in fluid mechanics, elasticity, electrical networks, chemical reactions, and many other areas of physical importance [38–42].

There is no unique definition of stiffness in the literature. However, essential properties of stiff systems are as follows: There exist, for certain initial conditions, solutions that change slowly and also solutions in a neighborhood of these smooth solutions converge quickly to them.

Although there are some attempts to solve stiff ordinary differential equations [26-29], but stiff terms in second order ordinary differential equations may cause large computation time due to high frequency oscillations. Stiff spring method eliminates these high frequency solution components in the dynamical simulation of multibody systems by adopting proper boundary condition. The increasing complexity of models in technical simulation may cause substantial problems in time integration. High frequency oscillations with very small amplitudes may be considered as a typical example of model components that are not relevant from the viewpoint of practical application but cause stability problems in explicit time integration methods and may slow down implicit integrators because of convergence problems in the corrector iteration.

In MBR due to the fact that there are discontinuities in the concentration profile at the boundaries between liquid and membrane phases, we have used three separate variables to describe the concentration in the respective phases. To get continuous flux over the phase boundaries, a special type of boundary conditions was applied using the stiff-spring method. Instead of defining Dirichlet concentration conditions according to the partition coefficient k,

which would destroy the continuity of the flux, continuous flux conditions were defined in which, at the same time, force the concentrations to the desired values:

$(-D'_{ds}\nabla c_M).n = M(c_{sh} - kc_M)$ at r=r_2 (inside the membrane side) (29)

$(-D''_{ds}\nabla c_{sh} + c_{sh}u).n = M(kc_M - c_{sh})$ at r=r_2 (inside the shell side) (30)

Here M is a (nonphysical) velocity large enough to let the concentration differences in the brackets approach zero thereby satisfying eq.12 and 16. These boundary conditions also give a continuous flux across the interfaces provided that M is sufficiently large.

4. Results and discussion

From the stability theory it became obvious that one has to use implicit methods for stiff problems. The goal of this study was assigned to define implicit methods that have a reduced computational complexity but on the other hand, it should be still accurate and stable. For stiff PDE, where the solution shows large variations over small intervals, some numerical methods are only stable when a very small step size is used. The concept of stiff spring integration has been applied to solve PDE governing equations of hollow fiber MBR in water treatment of diluted species.

4.1. Case study of model solving for Nitrate fluxes in the extractive MBR

We have solved the governing equations for denitrification of water. System specifications and physical conditions for nitrate removal by the extractive MBR to solve the governing equations with the given boundary conditions are listed in Table 1.

The vectors of total fluxes (diffusive and convective) of NO_3^- in the lumen, membrane and shell sides are illustrated in fig.3. Also, it presents the profiles of NO_3^- concentration (colored surfaces). The concentration of NO_3^- in the feed phase at one side of contactor, z=0 is at its maximum value and flow direction is from this point. As the feed flows through the tube side due to the presence of concentration gradient, the solute moves towards the membrane and its concentration is decreased along the fiber length in the lumen side. Fig.4 also shows a 3D view of concentration profile in the three sides.

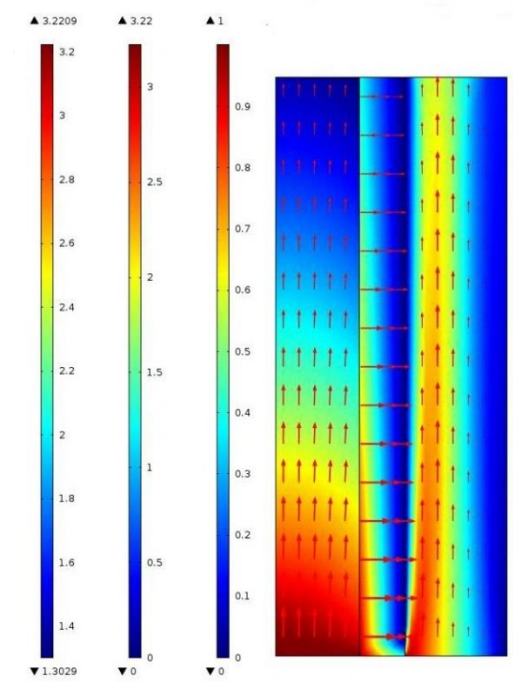

Fig.3 Total fluxes of NO^{3-} in the lumen, membrane and shell sides (vectors) and the profiles of NO^{3-} concentration (colored surfaces)

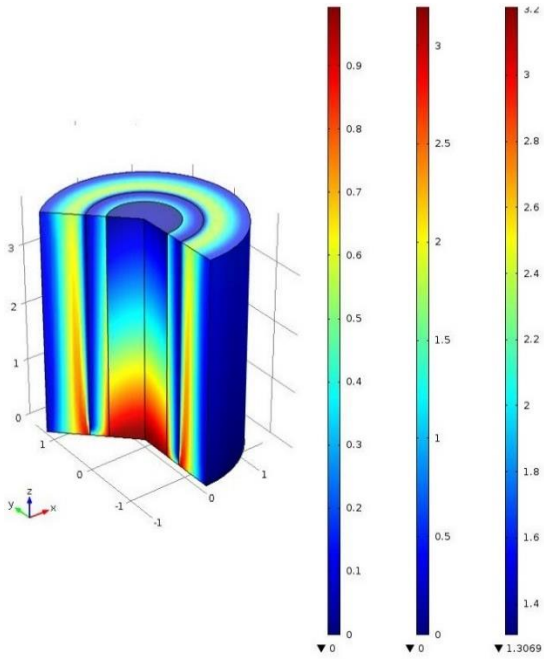

Fig.4A 3D view concentration profile in the lumen, membrane and shell side

Table 1. Parameters used in the model development

Model parameters	Value	Model parameters	Value
Dds (cm^2/s)	1.5×10^{-5}	C_0 (mg $NO^{3-}-N$ l^{-1})	200
ε	0.5	Q_{res} (ml min^{-1})	320
K_r	0.9	V_{res} (L)	1
r_1 (m)	5.5×10^{-4}	p_0 (atm)	1
r_2 (m)	8.5×10^{-4}	ρ (g/cm3)	1
r_3 (m)	1.52×10^{-3}	η (kg/m.s)	1.0×10^{-6}
L (m)	0.38		

4.2. Velocity field in the shell side

The surface velocity profile of NO_3^- in the shell side of membrane bioreactor is shown in fig. 5. Simulation results indicate that the velocity profile is almost parabolic due to the proximate permeation of NO_3^- . The results also reveal the effect of viscous forces at the region adjacent the shell wall. The effect of viscous force in these regions is significant and causes zero velocity (no slip) at the shell wall. The model considers the entry effects on the hydrodynamics of fluid flow in the shell side. At the inlet regions, the velocity profile is not developed. After a short distance from the inlet, the velocity profile is fully developed.

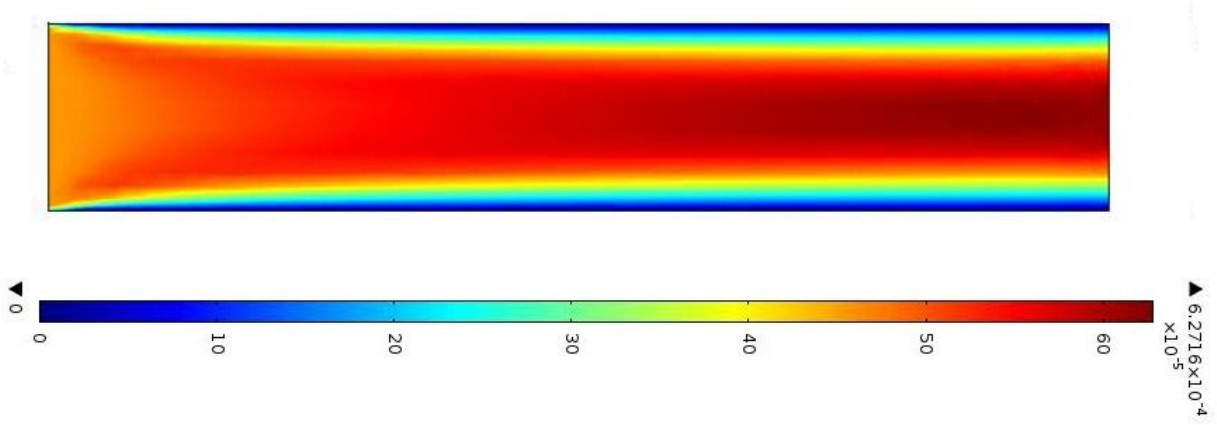

Fig. 5. The velocity field in the shell side of the extractive MBR

4.3. MBR efficiency

The MBR efficiency in the lumen is defined as:

$$Yeild = \frac{Q(c_L(0,r,t)-c_L(L,r,t))}{Qc_L(0,r,t)} \quad (33)$$

The effect of feed flow rate on the membrane efficiency is plotted in fig.6. By an increasing in the feed flow rate, the residence time of feed in the lumen decreases and consequently, the efficiency of purification and the total mass transfer of NO_3^- from the lumen to the shell side is reduced.

4.4. Effect of partition coefficient on membrane efficiency and exit concentration of lumen

The effect of partition coefficient on membrane efficiency with and without using stiff-spring method has been sketched in fig.7 and fig.8, respectively. The value of partition coefficient which is defined as the distribution of the solute between the feed and the solvent phase at equilibrium, can affect our output results in non-stiff method as illustrated in Fig. 8, while, by using stiff spring method the membrane efficiency does not fluctuated and it is completely stable (Fig.7). As results indicate in Fig. 8, for low values of partition coefficient, the membrane efficiency is negative which is not possible.

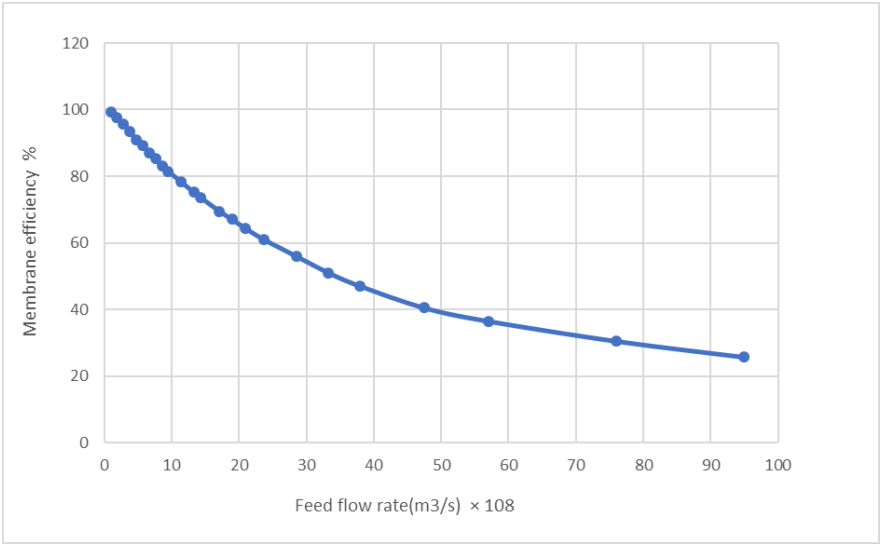

Fig. 6 The effect of feed flow rate on membrane efficiency

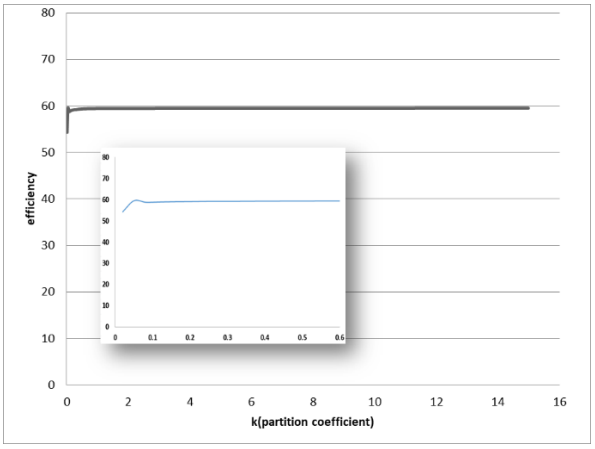

Fig. 7 Effect of partition coefficient on membrane efficiency using stiff-spring method

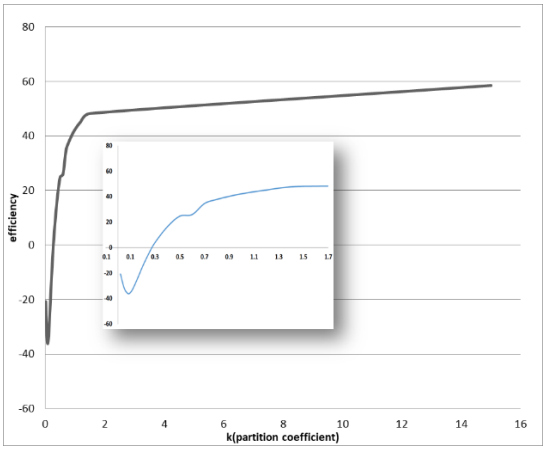

Fig.8 Effect of partition coefficient on membrane efficiency using non-stiff method

Simulation results in Fig. 8 show that, to achieve converge solution of PDEs extracted from mass balance equations and obtain the correct efficiency and exit concentration, a suitable value for the partition coefficient should be selected. But as we discussed earlier, partition coefficient is based on the choice of membrane properties and is justified by experiment. On the other hand, Fig. 7 shows that by applying stiff-spring method there aren't any worries about the solving of partial differential equations of the model. It means that they didn't diverge for any value of partition coefficient.

In some membrane operations like dialysis which the diffusion coefficient and their partition coefficient are small and cause an unnecessarily high membrane resistance [10]. Therefore, low values of k could affect the oscillations of convergence of the partial differential equations. As we see in fig.8 we have negative efficiency in low partition coefficient and even not accurate results up to the value of 15.

The effect of partition coefficient on the exit concentration of NO_3^- in the lumen side with and without using stiff spring method is illustrated in Fig. 9. From the results it can be concluded that at low values of partition coefficient, in non-stiff method, the value of exit concentration is greater than the inlet value which is not possible. On the other hand, the exit concentration of NO_3^- in the lumen is always less than the inlet concentration and from simulation results, the reasonable values are achievable when the stiff-spring method is used

in PDEs solution. In addition, the stiff-spring method could omit the umbrages of variations of partition coefficient due to the discontinuity of concentrations in the boundary conditions.

4.5. Model validation

The unsteady state equations of concentration of diluted species have been solved to predict the concentration profile of NO_3^- in the shell side of the membrane bio reactor by the method of stiff-spring. The model data showed a linear relationship when plotted in the form of φ vs. t, where φ=Ln[C0/(C0−c_{sh})]. For validating the simulated results, the experimental data from a previous work reported by Ergas and Rheinheimer [30] is used and comparison results is shown in fig. 10. As it is shown in Fig. 10, the trend of simulation results have a good agreement with the experimental data. Results confirms that the application of SSM in simulation is more reliable and accurate compare to non-stiff spring method.

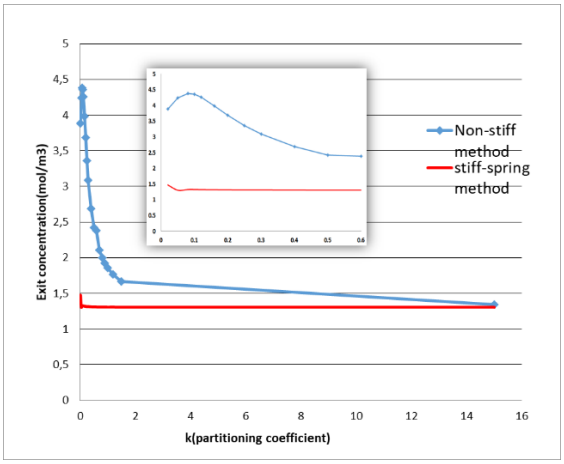

Fig. 9. the effect of partitioning coefficient on exit concentration of lumen

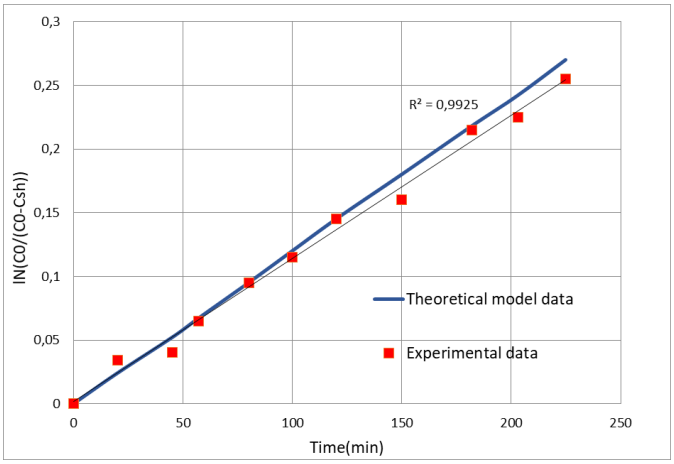

Fig. 10. A comparison between theoretical stiff-spring method and experimental data

5. Conclusion

In this paper, we have introduced a combination of finite element method and new stiff-spring method for stiff problem of governed mass conservation PDE equation of hollow fiber MBR. We have discussed the methodology for the construction of these schemes and investigated their performance on several characteristics of hollow fiber MBR. The solution is very rapidly convergent by utilizing new stiff spring method. From the stability theory it became obvious that one has to usually use implicit methods for stiff problems. The goal of this study was assigned to define implicit methods that reduce the computational complexity and at the same time be still accurate and stable. For stiff PDE equation sets, where the solution shows large variations over small intervals, some numerical methods are only stable when a very small step size is used.

This method also typically achieved long-time accuracy while circumventing the stringent stability restrictions on the time-step incurred by standard explicit. A comparison has been down between stiff and non-stiff methods and we showed that in some cases there are difficulties when using non-stiff method. For instance, exit concentration of lumen side was more than the inlet one for the low values of k and this is not possible. It means that the convergence and the accuracy of partial differential equations solution in the membrane is dependent on the value of partition coefficient and the stiff-spring method omits this dependency. On the other hand, the most usefulness of the stiff-spring method is in the membrane operations that the partition coefficient is varied according to concentration profiles. It could be possible to investigate and modify the effect of parameters which affect the MBR performance.

Nomenclatures

Parameter	Dimension	Description
c_L	(mol/m^3)	Diluted species concentration in the lumen
D_{ds}	$\left(m^2/s\right)$	Correlated diluted species diffusion coefficient in the lumen
R	$(mol/m^3 s)$	Rate of extraction of diluted species in the lumen
V_Z	(m/s)	Fluid velocity in the lumen
$\bar{u}$	(m/s)	Fluid average velocity in the lumen
C_0	(mol/m^3)	Inlet diluted species concentration in the lumen
c_M	(mol/m^3)	Diluted species concentration in the membrane
D'_{ds}	$\left(m^2/s\right)$	Correlated diluted species diffusion coefficient in the membrane (the effective diffusivity)
K_r	$dimensionless$	Restrictive factor
N	$(mol/m^2 s)$	Fluid flux
c_{sh}	(mol/m^3)	Diluted species concentration in the shell
D''_{ds}	$\left(m^2/s\right)$	Diluted species diffusion coefficient in the shell
R''	$(mol/m^3 s)$	Rate of extraction of diluted species in the shell
V''_Z	(m/s)	Fluid velocity in the shell
k		partition coefficient
p_0	(Pa)	Outlet pressure in the shell
$s(t)$	(mol/m^3)	Inlet diluted species concentration in the shell
$V''_{Z,0}$	(m/s)	Inlet fluid velocity in the shell
V_{res}	(m/s)	volume of the reservoir
Q	$\left(m^3/s\right)$	lumen side flow rate
Q_{res}	$\left(m^3/s\right)$	reservoir volumetric rate
a	$dimensionless$	Constant
d	(m)	Fiber diameter
D_{ds}	$\left(m^2/s\right)$	Diluted species diffusion coefficient (ordinary diffusion coefficient)
L	(m)	Fiber length
l	(m)	Fiber web thickness
n	$dimensionless$	Constant
r	(m)	Radial coordinate
r_1	(m)	Inner radius of the fiber
r_2	(m)	Outer radius of the fiber
r_3	(m)	Radius of the shell
t	(s)	Time
z	(m)	Axial coordinate
Greek letters		
ε	$dimensionless$	Fractional porosity
τ	$dimensionless$	Pore-path tortuosity
ε_p	$dimensionless$	Percolation threshold
τ_b	$dimensionless$	Bulk tortuosity
κ	$dimensionless$	Equilibrium partition coefficient
ρ	kg/m^3	Liquid density
η	$kg/m.s$	Dynamic viscosity
Abbreviations		
CFD		Computational fluid dynamics
FEA		Finite element analysis
MBR		Membrane bioreactor
HFMC		Hollow fiber membrane contactor

References

[1] Sondhi R, Bhave R and Jung G. Applications and benefits of ceramic membranes. Membr. Technol., 2003; 11: 5–8.

[2] Judd S. The MBR Book: Principles and Applications of Membrane Bioreactors in Water and Wastewater Treatment. Elsevier, Amsterdam; Boston; London, 2006.

[3] Stephenson T. Membrane Bioreactors for Wastewater Treatment. IWA, London, 2000.

[4] Shirazian S, Ashrafizadeh SN. Mass transfer simulation of carbon dioxide absorption in a hollow-fiber membrane contactor. Sep. Sci. Technol., 2010; 45:515–524.

[5] Shirazian S, Ashrafizadeh SN. Mass transfer simulation of caffeine extraction by subcritical CO_2 in a hollow-fiber membrane contactor. Solvent Extr. Ion Exch., 2010; 28: 267–286.

[6] Shirazian S, Moghadassi A, Moradi S. Numerical simulation of mass transfer in gas–liquid hollow fiber membrane contactors for laminar flow conditions. Simul. Modell. Pract. Theory, 2009; 17: 708–718.

[7] Afrane G, Chimowitz EH. Experimental investigation of a new super critical fluid-inorganic membrane separation process. J. Membr. Sci., 1996; 116: 293–299.

[8] Estay H, Bocquet S, Romero J, Sanchez J, Rios GM, Valenzuela F. Modeling and simulation of mass transfer in near-critical extraction using a hollow fiber membrane contactor. Chem Eng Sci., 2007; 62: 5794–5808.

[9] Sarrade S, Guizard C, Rios GM. Membrane technology and super critical fluids: chemical engineering for coupled processes. Desalination, 2002; 144: 137–142.

[10] Noble RD, Stern SA. Membrane separations technology principles and applications. Elsevier Science, 1999,472 .

[11] Xia XR, Baynes RE, Monteiro-Riviere NA, Riviere JE. Determination of the partition coefficients and absorption kinetic parameters of chemicals in a lipophilic membrane/water system by using a membrane-coated fiber technique. Euro J. Pharm Sci., 2005; 24: 15-23.

[12] Sanaeepur H, Hosseinkhani O, Kargari A, Amooghin AE, Raisi A. Mathematical modeling of a time-dependent extractive membrane bioreactor for denitrification of drinking water. Desalination, 2012; 289: 58–65.

[13] Rezakazemi M. Simulation of ammonia removal from industrial wastewater streams by means of a hollow-fiber membrane contactor. Desalination, 2012; 285: 383–392.

[14] Schwinge J, Neal PR, Wiley DE, Fletcher DF, Fane AG. Spiral wound modules and spacers. Review and analysis. J. Membr. Sci., 2004; 242: 129–153.

[15] Fimbres-Weihs GA, Wiley DE. Review of 3D CFD modeling of flow and mass transfer in narrow spacer-filled channels in membrane modules. Chem. Eng. Process., 2010; 49: 759–781.

[16] Ghidossi R, Veyret D, Moulin P. Computational fluid dynamics applied to membranes:state of the art and opportunities, Chem. Eng. Process.,2006; 45: 437–454.

[17] Li YL, Lin PJ, Tung KL. CFD analysis of fluid flow through a spacer-filled disk type membrane module. Desalination, 2011; 283: 140-147.

[18] Tung KL, Li YL, Hu CC, Chen YS. Power-law polymer solution flow in a converging annular spinneret: analytical approximation and numerical computation. AICHE J., 2012; 58: 122-131.

[19] Ghadiri M, Shirazian S. Computational simulation of mass transfer in extraction of alkali metals by means of nanoporous membrane extractors. Chem. Eng. Process, 2013; 69: 57-62.

[20] Ghadiri M, Marjani A, Shirazian S. Mathematical modeling and simulation of CO_2 stripping from monoethanolamine solution using nanoporous membrane contactors. Int. J. Greenh. Gas Con., 2013;13: 1–8.

[21] Ghadiri M, Fakhri S, Shirazian S. Modeling and CFD simulation of water desalination using nanoporous membrane contactors. Ind. Eng. Chem. Research, 2013; 52: 3490–3498.

[22] Ghadiri M, Fakhri S, Shirazian S. Modeling of water transport through nanopores of membranes in direct-contact membrane distillation process. Polym. Eng. Sci., 2014; 54: 660-666

[23] Ghadiri M, Darehnaei MG, Sabbaghian S, Shirazian S. Computational simulation for transport of priority organic pollutants through nanoporous membranes. Chem. Eng. Technol., 2013; 36: 507–512.

[24] Ghadiri M, Shirazian S, Ashrafizadeh SN. Mass transfer simulation of gold extraction in membrane extractors. Chem. Eng. Technol., 2012; 35: 2177–2182.

[25] Ranjbar M, Shirazian S, Parto SG, Ahmadi M. Computational fluid dynamics simulation of mass transfer in the separation of fermentation products using nanoporous membranes. Chem. Eng. Technol., 2013; 36: 728–732.

[26] Stabrowski MM. An efficient algorithm for solving stiff ordinary differential Equations. Simul. Modell. Pract. Theory, 1997; 5: 333-344.
[27] Metzger M. A comparative evaluation of DRE integration algorithms for real-time simulation of biologically activated sludge process. Simul. Modell. Pract. Theory, 2000; 7: 629-643.
[28] Castro R, Kofman E, Cellier FE. Quantization-based integration methods for delay-differential equations. Simul. Modell. Pract. Theory, 2011; 19: 314–336.
[29] Migoni G, Bortolotto M, Kofman E, Cellier FE. Linearly implicit quantization-based integration methods for stiff ordinary differential equations. Simul. Modell. Pract. Theory, 2013; 35: 118-136.
[30] Ergas SJ, Rheinheimer DE. Drinking water denitrification using a membrane bioreactor. Water Res., 2004; 38: 3225–3232.
[31] Koponen A, Kataja M, Timonen J. Simulations of single-fluid flow in porous medium, Int. J. Mod. Phys., 1998; 9: 1505–1521.
[32] L. André, H. Pauwels, M.-C. Dictor, M. Parmentier, M. Azaroual, Experiments and numerical modelling of microbially-catalysed denitrification reactions, Chem. Geol. 287 (2011) 171-181.
[33] Mulder M. Basic principle of membrane technology, Kluwer Academic Publisher, 1996, 399.
[34] Bird RB, Stewart WE, Lightfoot EN. Transport Phenomena. 2nd ed. John Wiley & Sons, New York, 1960.
[35] Happel J. Viscous flow relative to arrays of cylinders. AIChE J., 1959; 5: 174–177.
[36] Marcos B, Moresoli Ch, Skorepova J, Vaughan B. CFD modeling of a transient hollow fiber ultrafiltration system for protein concentration. J. Membr. Sci., 2009; 337: 136–144.
[37] Comsol, AB COMSOL Multiphysics Chemical Engineering Module Model Library, version 3.4, COMSOL AB, 2007.
[38] Flaherty JE, OMalley RE. The numerical solution of boundary value problems for stiff differential equations. Math. Comput., 1997; 31: 66 – 93.
[39] Bui TD, Bui TR. Numerical methods for extremely stiff systems of ordinary differential equations. Appl. Math. Modell., 1979; 3: 355 – 358.
[40] Butcher JC. Numerical Methods for Ordinary Differential Equations. Wiley, New York, 2003.
[41] Ixaru LGr, Berghe GV, de Meyer H. Frequency evaluation in exponential fitting multistep algorithms for ODEs. J. Comput. Appl. Math., 2000; 140: 423 – 434.
[42] Kaps P. Rosenbrock-type methods. in: G. Dahlquist, R. Jeltsch, (Eds.), Numerical methods for stiff initial value problems, Berich Nr. 9, Inst. Fur Geometric und Practische Mathematik der RWTH Aachen, 1981.

To whom correspondence should be addressed: Dr. M. Koolivand- Salooki, Gas Research Division, Research Institute of Petroleum Industry, Tehran, Iran, mehdi.koolivand@ut.ac.ir